BIOCHEMISTRY
including biophysical chemistry & molecular biology
Article

Biochemistry **2009,** *48,* 5417–5425 5417
DOI: 10.1021/bi9003974

Relocation of the Distal Histidine in Cytochrome *c* Peroxidase: Properties of CcP(W51H), CcP(W51H/H52W), and CcP(W51H/H52L)†

Miriam C. Foshay, Lidia B. Vitello, and James E. Erman*

Department of Chemistry and Biochemistry, Northern Illinois University, DeKalb, Illinois 60115

Received March 9, 2009; Revised Manuscript Received April 22, 2009

ABSTRACT: Many heme proteins have distal histidine residues that play important roles in determining heme protein reactivity. These distal histidines are in significantly different orientations,and distances from the heme iron in different heme proteins and the position of the distal histidine relative to the heme iron can influence reactivity at the heme center. To explore the effect of distal histidine position on the properties of cytochrome *c* peroxidase (CcP), three CcP mutants in which tryptophan 51 was replaced with a histidine residue were constructed. All three mutants, CcP(W51H), CcP(W51H/H52W), and CcP(W51H/H52L), have altered electronic absorption spectra, indicating that the heme group in the mutants is six-coordinate rather than five-coordinate as it is in wild-type CcP. The hydrogen peroxide reaction rate is 56−6200-fold slower for the mutants than for wild-type CcP. All three mutants form a CcP Compound I-like intermediate, in which the Fe(IV) site decays between 500 and 3000 times more rapidly than the Fe(IV) site in wild-type CcP Compound I. The W51H mutations have a weaker effect on cyanide binding, with the cyanide affinity only 2−8 times weaker than for CcP. The cyanide association rate constants are between 5 and 85 times slower for the W51H mutants, while the cyanide dissociation rate constants range from 3 times slower to 6 times faster than those of wild-type CcP.

Cytochrome *c* peroxidase (CcP),[1] a heme protein found in the yeast *Saccharomyces cerevisiae*, belongs to a superfamily of peroxidases and catalase-peroxidases, all of which have similar structure in the distal pocket above the heme. CcP is a part of Class I, which includes the ascorbate peroxidases of higher plants and green algae, and the catalase-peroxidases of bacteria and lower eukaryotes. Of 12 ascorbate peroxidases and 15 catalase-peroxidases investigated, all have the same amino acid sequence in the distal heme pocket, Arg-X-X-Trp-His (*1*), with one exception, the ascorbate peroxidase from *Mesembryanthemum crystallinum* that has a phenylalanine in place of tryptophan.

A comparison of the properties of metmyoglobin (metMb) and CcP is useful in trying to understand the role of the amino acid residues within the heme pockets of both proteins. CcP and metMb are similar in that both have a heme b prosthetic group ligated to the N_ε atom of a histidine residue in the proximal heme pocket and both proteins have distal histidine residues, His-64 in metMb and His-52 in CcP (*2*, *3*). However, there are significant differences. The proximal histidine in CcP, His-175, is hydrogen bonded to the carboxylate group of Asp-235, while the proximal histidine in metMb, His-93, is hydrogen bonded to the peptide carbonyl of Leu-80. The distal pocket of CcP is more polar than that of metMb with Arg-48, Trp-51, and His-52 nearest the heme iron in CcP compared to Phe-43, His-64, and Val-68 in metMb.

Peroxidases are characterized by a very rapid reaction with hydrogen peroxide that produces an intermediate called Compound I, which is oxidized 2 equiv above the native Fe(III) state of the enzyme. In most peroxidases, such as horseradish peroxidase (HRP), Compound I is an oxyferryl porphyrin π-cation radical species, while in CcP, the radical is localized on Trp-191, near the proximal histidine (*4*, *5*). MetMb also reacts with hydrogen peroxide to form a Compound I-like intermediate with an oxyferryl group and a transient radical that decays rapidly (*6*). However, metMb reacts 5 orders of magnitude more slowly than the peroxidases. Several studies using site-directed mutagenesis have probed the role of individual residues in the proximal and distal heme pockets of the peroxidases and have found that replacing the distal histidine with an apolar residue has the most profound effect, with CcP(H52L), HRP(H42A), and HRP(H42V) reacting 5−6 orders of magnitude more slowly

†This work was supported in part by the National Institutes of Health through Grant R15 GM59740.

*To whom correspondence should be addressed. Phone: (815) 753-6867. Fax: (815) 753-4802. E-mail: jerman@niu.edu.

[1]Abbreviations: CcP, generic abbreviation for cytochrome *c* peroxidase whatever the source; yCcP, authentic yeast cytochrome *c* peroxidase isolated from *Saccharomyces cerevisiae*; CcP(MI), recombinant CcP expressed in *Escherichia coli* with four amino acid variations compared to yCcP, a Met-Ile N-terminal extension, and mutations T53I and D152G; HRP, horseradish peroxidase; metMb, metmyoglobin, the Fe(III) form of myoglobin; rCcP, recombinant cytochrome *c* peroxidase expressed in *E. coli*. The rCcP used in this study has an amino acid sequence identical to that of yCcP. Mutations in the amino acid sequences of CcP are indicated by using the one-letter code for the amino acid residue in the wild-type protein, followed by the residue number and the one-letter code for the amino acid residue in the mutant protein. For example, CcP(W51H) represents a mutant in which a histidine residue replaces the tryptophan residue at position 51 of the wild-type protein; likewise, CcP(W51H/H52L) and CcP(W51H/H52W) represent double mutants in which alternative residues occur at both positions 51 and 52 of CcP.

Published on Web 04/23/2009

than wild-type CcP or HRP (*7*−*9*). On the other hand, the distal histidine in metMb seems to play a minor role in the reaction with hydrogen peroxide. Brittain et al. (*10*) observed a 1−2 order of magnitude decrease in the hydrogen peroxide reaction rate for the H64A and H64V mutants of sperm whale metMb and a 3-fold increase in the rate for the H64Q mutation.

The distal histidine in CcP is directly over the heme iron with an N_ε−Fe distance 5.6 Å (*3*). Compared to CcP, the distal histidine in sperm whale metMb is off-center and slightly closer to the heme with an N_ε−Fe distance 4.3 Å (*4*). Watanabe and co-workers (*11*, *12*) speculated that the distal histidine−iron distance is critical to efficient hydrogen peroxide reduction and tested that hypothesis by constructing two metMb double mutants, F43H/H64L and L29H/H64L, that moved the histidine N_ε atom 5.7 and 6.6 Å away from the heme iron, respectively. The F43H/H64L mutant had an N_ε−Fe distance similar to that of CcP and increased the hydrogen peroxide reaction rate 11-fold. The L29H/H64L mutant, with the 6.6 Å N_ε−Fe distance, reacted 3−6 times slower with hydrogen peroxide compared to wild-type metMb.

In this work, we relocate the distal histidine in CcP in studies similar to those of Watanabe and co-workers for metMb (*11*, *12*). If CcP has evolved to facilitate the reaction with hydrogen peroxide, the distal histidine in wild-type CcP should be in a near optimal position to promote peroxide binding and oxygen−oxygen bond cleavage to form CcP Compound I. Any alteration in the position of the distal histidine would be expected to decrease the rate of Compound I formation. We have constructed CcP(W51H/H52W), which interchanges the positions of the distal histidine and tryptophan residues. Modeling of the active site suggests that the histidine N_ε−Fe distance decreases from 5.6 Å in wild-type CcP to 5.2 Å in W51H/H52W. As expected, the hydrogen peroxide reaction rate for the W51H/H52W mutant is slower than that of wild-type CcP, decreasing ~2.5 orders of magnitude. Relocation of the distal histidine in CcP has a much greater effect on the reaction with hydrogen peroxide than does the relocation of the distal histidine in metMb. We have also constructed two additional mutants, W51H and W51H/H52L, and characterized all three in terms of their spectroscopic properties, hydrogen peroxide reactivity, Compound I decay, and cyanide binding properties.

MATERIALS AND METHODS

Cloning, Expression, and Purification of CcP Mutants. J. Satterlee (Washington State University, Pullman, WA) kindly provided the expression system for the recombinant CcP (rCcP) used in this study (*13*). The CcP gene was modified to include an N-terminal methionine for bacterial expression and the exact amino acid sequence of mature baker's yeast CcP (*14*). The CcP gene was inserted into the multiple cloning site of Novagene vector pET24a(+) under control of the T7 promoter. The CcP mutants were created using the Stratagene QuikChange mutagenesis kit and sequenced in both directions to ensure that, except for the intended mutations, the gene was identical to the published sequence. Expression and purification of rCcP and the CcP mutants were performed as previously described (*15*−*18*).

Other Materials. Acetic acid, potassium acetate, potassium phosphate salts, potassium cyanide, and hydrogen peroxide (30%) were obtained from Fisher Scientific. Concentrations of hydrogen peroxide were determined in two ways: by titration with Ce(IV) as described previously (*19*) and from the absorbance at 240 nm using an extinction coefficient of 39.4 M^{-1} cm^{-1} (*20*).

Buffers. Between pH 4.0 and 5.5, buffers were 0.010 M acetate with sufficient KH_2PO_4 to adjust the ionic strength to 0.100 M. Between pH 5.5 and 8.0, the buffers were mixtures of KH_2PO_4 and K_2HPO_4 with a total ionic strength of 0.100 M.

Spectroscopic Measurements and Protein Concentration Determination. Spectra of protein solutions were determined using either a Varian/Cary model 3E or a Hewlett-Packard model 8452A spectrophotometer. The extinction coefficients of the four CcP mutants were determined using the pyridine hemochromogen method of Berry and Trumpower (*21*).

Kinetics of Compound I Formation. The rate of Compound I formation was determined under pseudo-first-order conditions, with peroxide concentrations ranging from 10- to 100-fold greater that the enzyme concentration. Concentrations of CcP and its mutants were typically between 1 and 2 μM. Transient-state kinetic experiments were performed with an Applied Photophysics DX.17MV stopped-flow spectrophotometer at 25 °C, using a wavelength of 424 nm, the wavelength of maximum change between Compound I and the native enzyme. The observed pseudo-first-order rate constant, k^{obs}, was determined at a minimum of five different concentrations of hydrogen peroxide. The apparent bimolecular rate constant, k_1, for the reaction between hydrogen peroxide and CcP (or its mutants) was determined from the slope of a plot of k^{obs} as a function of hydrogen peroxide concentration.

Kinetics of Compound I Decay. Compound I was formed using either 0.5, 1.0, or 2.0 equiv of hydrogen peroxide to enzyme to investigate the effects of excess hydrogen peroxide on the stability of Compound I. Conversion of Compound I back to the Fe(III) state was followed spectrophotometrically using the HP 8452A diode array spectrophotometer at 25 °C. Complete spectra were collected at 30−150 s intervals for at least 1 h or until the spectrum of the decay product stabilized.

Determination of the Equilibrium Constants for Cyanide Binding. Spectroscopic changes associated with the formation of the cyanide complex enabled monitoring of complex formation. Determination of the equilibrium constants was done by titrating ~5 μM protein with increasing concentrations of a buffered cyanide solution until saturation with cyanide was reached. The spectrum of the solution was determined after equilibrium had been reached at each cyanide concentration. Equilibrium constants were determined from changes in absorbance as a function of cyanide concentration at 25 °C.

Transient-State Kinetic Measurements of Cyanide Binding. The rates of cyanide binding were determined using an Applied Photophysics Ltd. model DX.17MV stopped-flow instrument at 25 °C. Reactions were conducted under pseudo-first-order conditions with excess cyanide. Protein concentrations were typically ~2 μM. Observed rate constants were determined at a minimum of five different cyanide concentrations at each pH with the cyanide concentrations varying by a factor of at least 5 for each experiment. A minimum of 10 individual traces of absorbance change versus time were acquired at each cyanide concentration, allowing the mean value of the observed rate constant and its standard deviation to be determined.

RESULTS

Spectroscopic Properties of CcP Variants. One of the most dramatic changes in the properties of the three W51H

mutants compared to wild-type CcP occurs in the electronic absorption spectrum (Figure 1). The Soret band becomes narrower and much more intense with the extinction coefficient increasing by ~60% in CcP(W51H) compared to that of rCcP. The spectral changes signal a change in heme coordination upon mutation of Trp-51 to a histidine residue. The spectrum of CcP (W51H) is characteristic of a predominantly hexacoordinate, high-spin heme protein, while the spectrum of rCcP is that of a predominantly five-coordinate, high-spin ferric heme protein (*22*). The spectrum of CcP(W51H) is similar to that of metmyoglobin, a ferric heme protein with water bound to the sixth coordination site of the heme iron (*23*), and we suggest that water binds to the heme iron in the W51H mutants. Spectroscopic parameters for rCcP and the three W51H mutants at pH 6.0 are collected in Table 1.

CcP and its mutants are generally stable between pH 4 and 8, and spectra for all three W51H mutants were recorded at pH 4.0, 6.0, and 8.0. The pH 4.0 spectra indicate that the three W51H mutants are significantly less stable at pH 4.0 than wild-type rCcP. When solutions of the W51H mutants are adjusted to pH 4.0, the intensity of the Soret maximum decreases significantly compared to its absorbance at pH 6.0, and the spectrum is time-dependent with continued loss of absorptivity in the Soret region. Because of the low stability of the W51H mutants at low pH, we have focused on the spectral properties between pH 6 and 8.

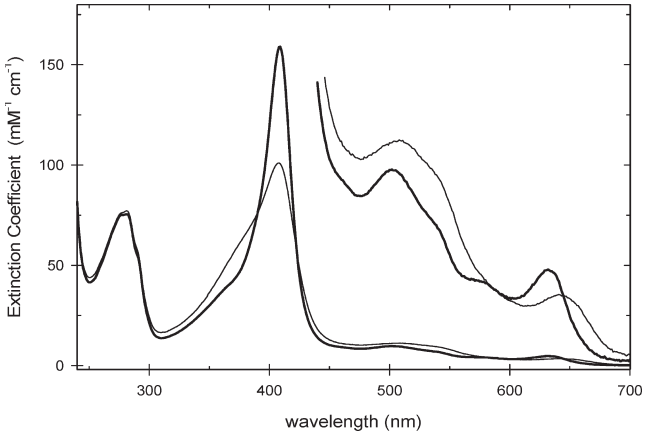

FIGURE 1: Absorption spectrum of CcP(W51H) (thick line) and rCcP (thin line) at pH 6, in a 0.10 M ionic strength potassium phosphate buffer, at 25 °C.

The spectra for CcP(W51H/H52L) at pH 6.0 and 8.0 are shown in Figure 2, while spectra for CcP(W51H) and CcP (W51H/H52W) are shown Figures S1 and S2 of the Supporting Information. Note that the spectrum of CcP(W51H/H52L) and CcP(W51H) are almost identical at pH 6.0 (Figures 1 and 2 and Table 1). Comparison of the spectra of the mutants at pH 6.0 and 8.0 indicates that the heme-bound water ionizes in this pH region and that the pH 8.0 spectra are those of the predominantly hydroxyl-ligated mutants with a six-coordinate, low-spin ferric heme group. Spectral parameters for the three mutants at pH 8.0 are included in Table 1.

Reaction of the CcP Mutants with Hydrogen Peroxide. Addition of excess hydrogen peroxide to CcP(W51H) at pH 6.0 causes formation of an oxidized intermediate with spectroscopic characteristics similar to those of yeast CcP Compound I (Figure 3). CcP(W51H) Compound I has α, β, and Soret bands at 558, 530, and 416 nm, respectively, compared to rCcP Compound I, which has α, β, and Soret bands at 560, 530, and 420 nm, respectively. The extinction coefficients at the maxima are also similar (Table 1). For reasons to be presented later, the spectrum of CcP(W51H) Compound I shown in Figure 3 was corrected for ~15% Compound I decay.

The rate of reaction between the W51H mutants and hydrogen peroxide was investigated using stopped-flow techniques. The reactions of all three mutants were biphasic with the major phase of the reaction accounting for 80−88% of the reaction amplitude at 424 nm. Figure 4 shows a plot of the absorbance change at 424 nm upon addition of 21.0 μM H_2O_2 to 2.25 μM CcP(W51H) at pH 6.0. The formation of CcP(W51H) Compound I is biphasic with the fast phase of the reaction contributing ~80% to the reaction amplitude. The observed rates were determined as a function of the H_2O_2 concentration (11−84 μM), and both increase linearly with an increasing H_2O_2 concentration (Figure 5). The slopes of the plots shown in Figure 5 give the apparent bimolecular rate constants for the reaction between CcP (W51H) and H_2O_2. The fast and slow phases of the reaction have bimolecular rate constants of $(8.5 \pm 0.1) \times 10^5$ and $(5.8 \pm 1.0) \times 10^4$ M^{-1} s^{-1}, respectively. These data are collected in Table 2 along with those of yCcP, rCcP, and other CcP mutants.

The reaction between CcP(W51H/H52W) and hydrogen peroxide shows a somewhat different pattern of reactivity compared to that of CcP(W51H). The reaction is biphasic, but in the case of CcP(W51H/H52W), the major phase of the reaction (86%) has the slower rate, with an apparent bimolecular rate constant of

Table 1: Peak Positions and Extinction Coefficients for the W51H Mutants of CcP and Their Cyanide Complexes[a]

protein	pH	protein band λ (ε)	δ band λ (ε)	Soret band λ (ε)	visible region λ (ε)
rCcP	6.0	281 (76)		408 (101)	508 (11.2), 641 (3.5)
CcP(W51H)	6.0	281 (76)		409 (159)	502 (9.8), 632 (4.8)
CcP(W51H/H52L)	6.0	281 (76)		408 (160)	502 (10.5), 633 (4.7)
CcP(W51H/H52W)	6.0	278 (90)		409 (137)	526 (9.5), 632 (3.1)
rCcP	8.0	281 (75)		410 (98)	515 (10.3), 639 (2.7)
CcP(W51H)	8.0	277 (75)		412 (119)	533 (10.2)
CcP(W51H/H52L)	8.0	278 (75)		410 (105)	533 (9.7)
CcP(W51H/H52W)	8.0	278 (88)		412 (111)	533 (10.5)
rCcP Compound I	6.0	278 (74)		420 (107)	530 (12.9), 560 (14.7)
CcP(W51H) Compound I	6.0			416 (115)	530 (12.8), 558 (13.4)
rCcP−CN	6.0	282 (83)	362 (34)	422 (117)	542 (13.4)
CcP(W51H)−CN	6.0	280 (74)	364 (34)	422 (112)	540 (13.0)
CcP(W51H/H52L)−CN	6.0	277 (80)	362 (39)	421 (112)	542 (12.6)
CcP(W51H/H52W)−CN	6.0	277 (91)	360 (32)	420 (109)	541 (13.1)

[a] λ, wavelength in nm. ε, extinction coefficient in M^{-1} cm^{-1}.

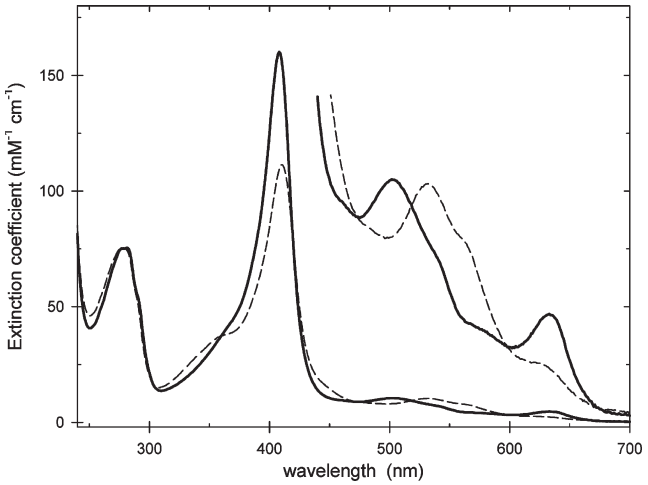

FIGURE 2: Spectra of CcP(W51H/H52L) at pH 6 (solid line) and pH 8 (dashed line). The visible regions of the spectra are shown multiplied by a factor of 10.

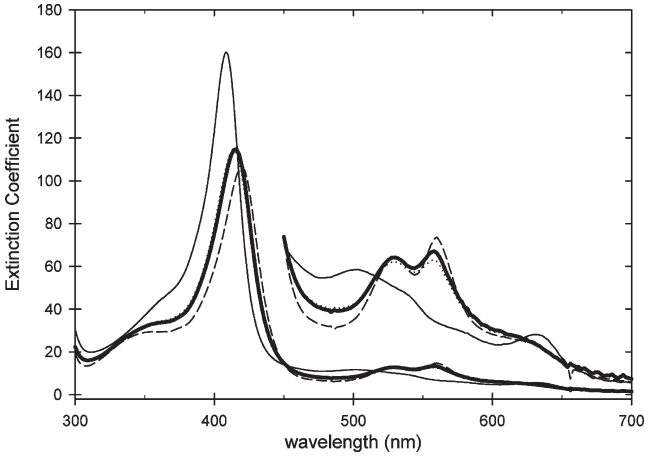

FIGURE 3: Spectra of CcP(W51H) (thin solid line), CcP(W51H) Compound I (thick solid line), and yCcP Compound I (dashed line). The visible regions of the spectra are shown multiplied by a factor of 5. The spectrum of CcP(W51H) Compound I was calculated from the initial spectrum acquired (dotted line) after manual mixing of 7.24 μM CcP(W51H) and 20.8 μM H_2O_2 (~10 s) by correcting for an estimated ~15% of decay product.

$(1.6 \pm 0.1) \times 10^5$ M^{-1} s^{-1}, while the minor phase of the reaction has the larger rate constant, $(8.6 \pm 3.4) \times 10^5$ M^{-1} s^{-1}.

CcP(W51H/H52L) shows a third pattern of reactivity. The reaction with hydrogen peroxide is much slower compared to those of the first two W51H mutants with the apparent second-order rate constant for the major phase (88%) of the reaction being only $(7.8 \pm 0.4) \times 10^3$ M^{-1} s^{-1} (Figure S4 of the Supporting Information). The minor phase of the CcP(W51H/H52L)/H_2O_2 reaction is independent of hydrogen peroxide concentration (Figure S5 of the Supporting Information), with an apparent first-order rate constant of (6 ± 3) s^{-1} (Table 2), quite different from the peroxide dependence of the minor phases of the reactions with CcP(W51H) and CcP(W51H/H52W).

The major, bimolecular phases of the reaction between the W51H mutants and hydrogen peroxide show significant decreases in the rate of reaction, with 56-, 300-, and 6200-fold decreases for CcP(W51H), CcP(W51H/H52W), and CcP(W51H/H52L), respectively, compared to that of rCcP, indicating that the position of the distal histidine has a significant effect on the rate of reaction with H_2O_2.

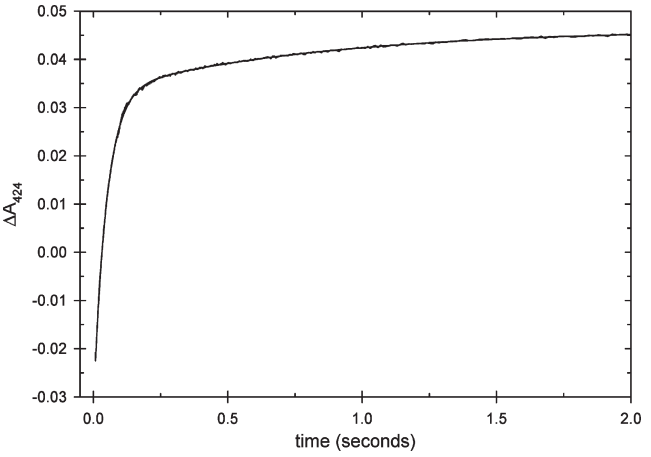

FIGURE 4: Absorbance change at 424 nm upon addition of 21 μM H_2O_2 to 2.25 μM CcP(W51H) at pH 6.0. Data were acquired between 7.55 ms and 50 s using a logarithmic time with the Applied Photophysics stopped-flow spectrophotometer; only the first 2 s of the data is shown, and these are shown on a linear time axis. The absorbance change is biphasic and was fit to the sum of two exponential curves. Nonlinear least-squares regression analysis gives best fit values of 20.9 ± 0.1 and 1.23 ± 0.03 s^{-1} for the observed pseudo-first-order rate constants and amplitude values of 0.0652 ± 0.0001 and 0.0132 ± 0.0001 for the fast and slow phases, respectively. Both the data and the regression line, which are superimposable, are shown.

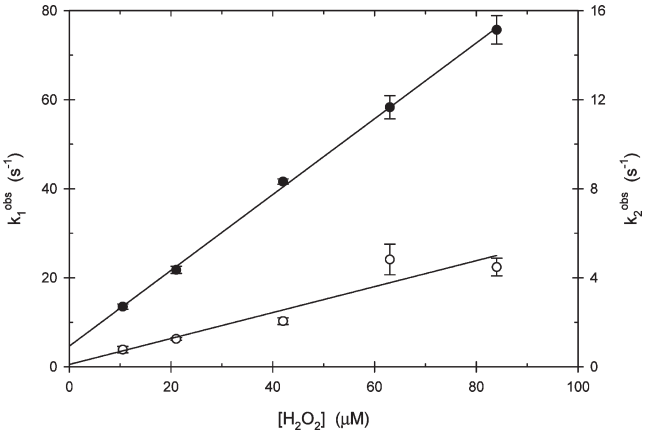

FIGURE 5: Plot of the observed rate constants for the CcP(W51H)/H_2O_2 reaction at pH 6.0 as a function of H_2O_2 concentration: fast major phase of the reaction, k_1^{obs} (●, left-hand axis), and slow minor phase of the reaction, k_2^{obs} (○, right-hand axis). The slopes of the plots give the apparent bimolecular rate constants, k_1^{app} and k_2^{app}, for the reaction between substrate and enzyme. These data are collected in Table 2 for both the major and minor phases of the reaction.

Decay of Compound I Formed by the W51H Mutants. Another profound difference between the W51H mutants and either yCcP or rCcP is that Compound I formed by the W51H mutants is significantly less stable than Compound I formed by yCcP (*24*). In addition, the pattern of endogenous reduction of the Fe(IV)=O heme and radical sites in Compound I of the W51H mutants is unique. Figure 6 shows the change in absorbance over a period of 1 h at 424 nm after addition of 2.07 equiv of H_2O_2 to CcP(W51H) at pH 6.0. The data are triphasic and were fit to a three-exponential decay curve using nonlinear least-squares regression. The fastest phase of the reaction is also the one that produces the largest decrease in absorbance at 424 nm and is attributed to reduction of the Fe(IV)=O heme in CcP (W51H) Compound I. Best-fit values for the decay rates and

Table 2: Rate Constants for Formation of Compound I from Selected CcP Mutants at pH 6.0

protein	k_1 (major phase) (M^{-1} s^{-1})	k_2 (minor phase)	% amplitude (major phase)
yCcP[a]	$(4.5 \pm 0.3) \times 10^7$		100
rCcP[a]	$(4.8 \pm 0.2) \times 10^7$	$(1.3 \pm 0.1) \times 10^6$ M^{-1} s^{-1}	82
W51H	$(8.5 \pm 0.1) \times 10^5$	$(5.8 \pm 1.0) \times 10^4$ M^{-1} s^{-1}	80
W51H/H52W	$(1.6 \pm 0.1) \times 10^5$	$(8.6 \pm 3.4) \times 10^5$ M^{-1} s^{-1}	86
W51H/H52L	$(7.8 \pm 0.4) \times 10^3$	6 ± 3 s^{-1}	88
H52L[b]	$(7.3 \pm 0.4) \times 10^2$		100

[a] Data from ref *35*. [b] Data from ref *8*.

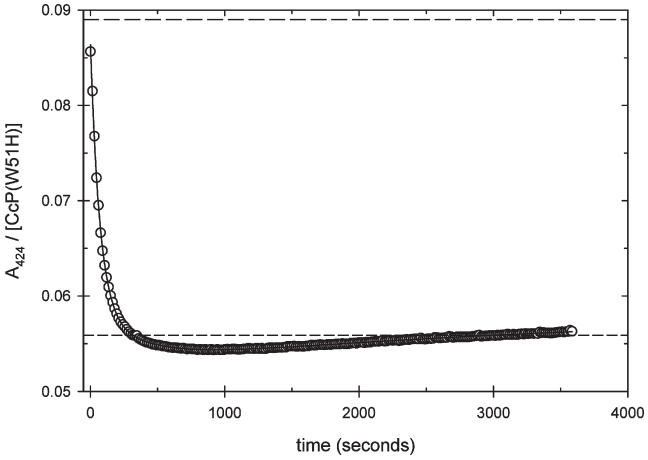

FIGURE 6: Decay of CcP(W51H) Compound I at pH 6.0. With respect to experimental conditions, 7.91 μM H_2O_2 was manually added to 3.82 μM CcP(W51H) (~10 s) and the absorbance at 424 nm was measured at 15 s intervals for a period of 1 h. The absorbance change was normalized to 1.00 μM enzyme. The upper and lower dashed lines represent the absorbance of 1 μM CcP(W51H) Compound I and CcP(W51H), respectively. The data were fit to a three-exponential decay curve using nonlinear least-squares regression.

amplitudes of the three phases are collected in Table 3. The observed amplitudes in Table 3 are expressed as the percent of the total absorbance change between Compound I and the native Fe (III) form of the enzyme. A negative sign indicates a decrease in absorbance at 424 nm, while a positive sign indicates an increase in absorbance. The latter two phases of CcP(W51H) Compound I decay are attributed to either reduction of the radical site or migration of the radical site away from the heme.

For CcP(W51H/H52W) and CcP(W51H/H52L), the rate of formation of Compound I is 5−100 times slower than for CcP (W51H) and the rate of decay is 2−6 times faster. As a consequence, when a stoichiometric amount of H_2O_2 is added to the two double mutants using manual mixing procedures, only ~20% of Compound I is formed for CcP(W51H/H52L) and 10% for CcP(W51H/H52W). The decay of Compound I for these two double mutants was followed at 424 nm for 1 h. The decay is biphasic with the fast phase, attributed to reduction of the Fe(IV) =O heme, causing a decrease in absorbance at 424 and the slow phase, attributed to radical reduction or migration away from the heme pocket, causing an increase in absorbance at 424 nm (Figure S6 of the Supporting Information). The small amplitude of the second phase of the decay reaction makes it difficult to obtain accurate values for the rate constant. In addition, there is some evidence that the rate may depend upon the initial ratio of H_2O_2 concentration to enzyme concentration used to generate Compound I. The kinetic parameters are collected in Table 3.

The rapidity of decay of the Fe(IV) site in all three mutants containing the W51H alteration makes determination of the Compound I spectrum difficult. The fastest rate of formation and the slowest rate of decay of Compound I are for CcP(W51H). The spectrum of CcP(W51H) Compound I, determined from manual mixing experiments, is shown in Figure 3. It is estimated that ~15% of the Fe(IV) site had decayed by the time the spectrum of CcP(W51H) Compound I was recorded. The rates of Compound I formation are slower for the double mutants (Table 2), and the decay of the Fe(IV) site is faster (Table 3); therefore, Compound I spectra were not obtained for the double mutants.

Spectroscopic Properties of Cyanide Binding to the CcP Mutants. Addition of buffered cyanide solutions to the three CcP mutants causes large changes in the absorption spectrum of the enzyme. Spectral changes associated with cyanide binding to CcP(W51H) at pH 6.0 are shown in Figure 7. Upon binding of cyanide, the Soret maximum of CcP(W51H) shifts from 409 to 422 nm with the extinction coefficient decreasing from 159 to 112 mM^{-1} cm^{-1}. The spectrum of the cyanide complex is typical of a six-coordinate, low-spin species with a prominent β band at 540 nm. The spectrum of the cyanide complex of rCcP is shown in Figure 7 for the sake of comparison. The spectra of the cyano complexes of the double CcP mutants are shown in Figures S7 and S8 of the Supporting Information and are similar to that shown in Figure 7. Spectral parameters for the cyanide complexes of all three CcP mutants are collected in Table 1.

Equilibrium Dissociation Constants for Binding of Cyanide to the CcP Mutants. Titration of the three W51H mutants with buffered cyanide solutions at pH 6.0 fit a simple one-to-one titration equation. The titration data for CcP(W51H) are shown in Figure 8. The absorbance was monitored at 428 nm, the wavelength of maximum absorbance change between cyanide-bound and cyanide-free CcP(W51H). The binding is quite strong, and the data were fit to the quadratic form of the one-to-one titration equation (eq 1).

$$\Delta A = \frac{\Delta A_\infty}{2E_T}\left[E_T + L_T + K_D^{equil} - \sqrt{(E_T + L_T + K_D^{equil})^2 - 4E_T L_T}\right] \quad (1)$$

where E_T and L_T are the total concentrations of enzyme and ligand in solution, respectively, ΔA_∞ is the maximum change in absorbance in the presence of an infinite concentration of ligand, and K_D^{equil} is the equilibrium dissociation constant for the cyanide complex. Best-fit values for ΔA_∞ and K_D^{equil} were determined using nonlinear least-squares regression. The best-fit value for K_D^{equil} in the experiment shown in Figure 8 is 14 ± 2 μM. The equilibrium dissociation constants for yCcP and the three W51H mutants are collected in Table 4. The affinity for cyanide is decreased 2−8-fold in the three W51H mutants compared to that in yCcP (*25*).

Kinetics of Binding of Cyanide to the CcP Mutants. The binding of cyanide to the CcP mutants was sufficiently fast that

Table 3: Kinetic Parameters for Compound I Decay for yCcP and the W51H Mutants[a]

	Fe(IV) site k_1^{decay} (s^{-1})	ΔA_1^{obs} (%)	radical site 1 k_2^{decay} (s^{-1})	ΔA_2^{obs} (%)	radical site 2 k_3^{decay} (s^{-1})	ΔA_3^{obs} (%)
yCcP[b]	$(2.9 \pm 0.6) \times 10^{-5}$	−80	$(1.3 \pm 0.3) \times 10^{-3}$	−20		
W51H	$(1.4 \pm 0.3) \times 10^{-2}$	−83	$(3.2 \pm 1.2) \times 10^{-3}$	−19	2×10^{-5} to 2×10^{-6}	+17
W51H/H52W	$(8.8 \pm 0.5) \times 10^{-2}$	−8			1×10^{-3} to 7×10^{-4}	+5
W51H/H52L	$(3.7 \pm 0.1) \times 10^{-2}$	−31			2×10^{-3} to 5×10^{-4}	+16

[a] At pH 6.0, 0.10 M ionic strength with potassium phosphate buffer, $[H_2O_2]$/[enzyme] ratio between 0.7 and 2.1. The observed amplitudes are expressed as the percent of the total absorbance change between Compound I and the native Fe(III) form of the enzyme. A negative sign indicates a decrease in absorbance at 424 nm for the decay process, while a positive sign indicates an increase in absorbance. [b] Data from ref *24*.

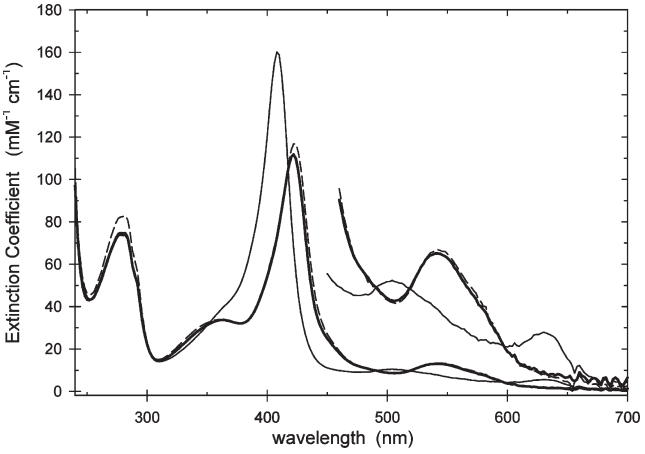

FIGURE 7: Spectra of CcP(W51H) (thin solid line), the CcP(W51H)−cyanide complex (thick solid line), and the rCcP−cyanide complex (dashed line) at pH 6.0. Spectroscopic parameters are listed in Table 1.

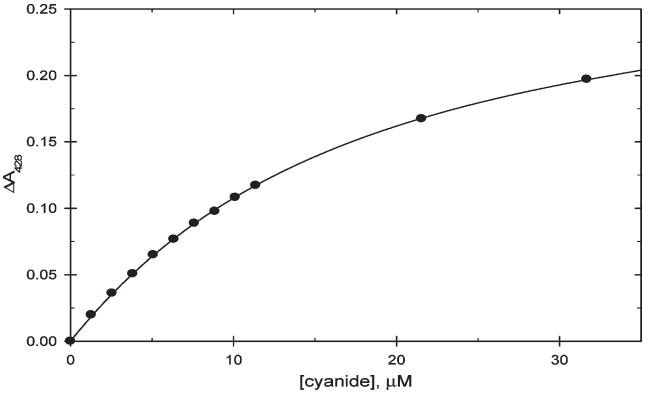

FIGURE 8: Titration of CcP(W51H) with cyanide at pH 6.0. A 5 μM solution of CcP(W51H) was titrated with small aliquots of buffered KCN. The absorbance changes at 428 nm were monitored and corrected for dilution. The data fit a simple one-to-one titration curve. Nonlinear least-squares regression gave a best-fit value for the equilibrium constant (K_D^{equil}) of 14 ± 2 μM.

the reaction was monitored by stopped-flow techniques. The reactions of cyanide with all three mutants are biphasic under all experimental conditions, and the observed rate constants are defined as k_{fast} and k_{slow} for the fast and show phases, respectively. The fast rate constant, k_{fast}, is linearly dependent upon the cyanide concentration, while k_{slow} is independent of cyanide concentration (Figure 9 and Figures S11 and S12 of the Supporting Information). Association and dissociation rate constants for cyanide binding, k_a and k_d, respectively, can be determined from the slopes and intercepts of the plots of k_{fast} as a function of the cyanide concentration shown in Figures 9, S11, and S12. The slow rate is attributed to an isomerization between two conformations of the enzyme. The values of k_a, k_d, and k_{slow} for the three CcP mutants are listed in Table 4 along with data for yCcP (*25*). The association rate constant is between 5 and 85 times slower for the mutants than for yCcP, while the dissociation rate constants are similar, ranging from 3 times slower to 6 faster compared to that of yCcP.

DISCUSSION

Spectroscopic Properties of CcP Variants. All heme proteins have four characteristic absorption bands defined as the α, β, γ (Soret), and δ bands in the visible and near-UV region of the electronic absorption spectrum (*26*, *27*). High-spin ferric heme proteins have two additional ligand-to-metal charge transfer bands designated CT1 and CT2 (*26*, *27*). Both the band position and the extinction coefficient are sensitive to the spin and coordination state of the ferric heme group, providing information about the nature of heme ligation. Heme protein spectra are often pH-dependent, indicating changes in heme coordination with changes in pH.

The CcP variants with the W51H mutation have dramatically altered absorption spectra compared to that of wild-type CcP, and at pH 6.0, their spectra are very similar to that of metmyoglobin (*23*). The spectra of the mutants are characteristic of a heme group with water bound at the sixth coordination site. Going from a five-coordinate heme to a six-coordinate heme increases the extinction coefficient at the Soret maximum by ~60%. The heme-bound water in CcP(W51H) and CcP(W51H/H52L) ionizes between pH 6 and 8, and the spectra at pH 8 are consistent with hydroxide ion binding to the heme iron (Table 1). At pH 4, the Soret band for all three mutants undergoes a loss of absorptivity, suggesting the beginning of acid denaturation, which is confirmed by the time dependence of the spectra.

Savenkova et al. (*28*) have made similar mutations in horseradish peroxidase, HRP, and did not observe significant changes in the spectrum of HRP as seen for the W51H mutants of CcP. The amino acid residues forming the distal heme pocket in HRP are Arg-38, Phe-41, and His-42, with Phe-41 in a position equivalent to that of Trp-51 in CcP. The extinction coefficient at the Soret maximum of HRP(F41H/H42A) is similar to that of wild-type HRP (*28*). However, metmyoglobin (metMb) mutants do show large perturbations of the absorption spectrum depending upon the presence or absence of heme-bound water. Brancaccio et al. (*29*) have shown that sperm whale metMb is five-coordinate when an apolar residue such as Val, Ile, Leu, or Phe is substituted for the distal histidine, His-64. Matsui et al. (*11*) show that while sperm whale metMb(H64L) has a substantially decreased Soret absorption compared to that of wild-type metMb, consistent with five-coordinate heme, double mutations that move the distal histidine to alternative locations within the distal heme pocket can restore the water binding to the heme.

Table 4: Equilibrium and Kinetic Parameters for Binding of Cyanide to the W51H Mutants of CcP[a]

	k_a (M^{-1} s^{-1})	k_d (s^{-1})	k_{slow} (s^{-1})	K_D^{kin} (μM)	K_{iso}	K_D^{equil} (μM)
yCcP[b]	$(1.1 \pm 0.1) \times 10^5$	0.39 ± 0.05		3.6 ± 0.6		6 ± 3
W51H	$(5.7 \pm 0.3) \times 10^3$	0.60 ± 0.04	0.36 ± 0.11	110 ± 10	0.15 ± 0.03	14 ± 2
W51H/H52W	$(2.1 \pm 0.1) \times 10^4$	2.5 ± 0.3	0.63 ± 0.18	120 ± 20	0.62 ± 0.21	46 ± 6
W51H/H52L	$(1.3 \pm 0.1) \times 10^3$	0.11 ± 0.03	0.16 ± 0.11	85 ± 24	0.60 ± 0.30	32 ± 4

[a] At pH 6.0 and 0.10 M ionic strength with potassium phosphate buffer. [b] From ref *25*.

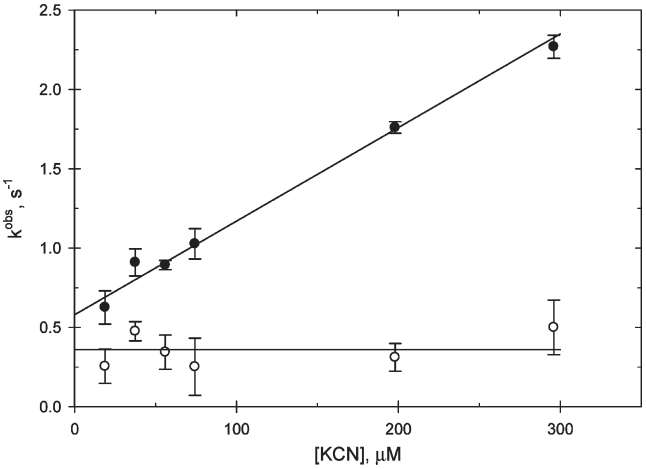

FIGURE 9: Plots of the observed rate constants for binding of cyanide to CcP(W51H) at pH 6.0: (●) observed rate constant, k_{fast}, for the major phase of the reaction and (○) observed rate constant, k_{slow}, for the minor phase of the reaction.

The spectra of metMb(L29H/H64L) and metMb(F43H/L64L) are similar to that of wild-type metMb, indicating heme-bound water.

Reaction of the CcP Mutants with Hydrogen Peroxide. A primary objective of this study was to determine if the location of the distal histidine residue within the distal heme pocket would have a significant effect on the rate of reaction with hydrogen peroxide. The answer is yes, with the three W51H mutants all reacting with H_2O_2 at reduced rates. The reduction varies from 56-fold for CcP(W51H) (which has two histidines in the heme pocket) to 6200-fold for the double mutant W51H/H52L. The reduction in rate is attributed to disruption of the hydrogen bonding network and the rearrangement of water molecules within the distal heme pocket. The W51H mutation allows water to bind to the heme iron at pH 6.0, and this ligation may be important in slowing the H_2O_2 reaction. If one assumes that the five- and six-coordinate forms of CcP are in rapid equilibrium and that H_2O_2 reacts with only the five-coordinate form, the observed rate constant for the mutants would be the bimolecular rate constant for the five-coordinate form times the fraction of enzyme in the five-coordinate form.

If the only effect of the W51H mutation in CcP(W51H) is to facilitate coordination of water to the heme iron, then an estimate of the equilibrium fraction of five-coordinate heme in this mutant can be made by multiplying the ratio of k_1 for CcP(W51H) to k_1 for rCcP by 100%. The estimated fraction of five-coordinate heme in CcP(W51H) is 1.8%. This estimate assumes that the W51H mutation does not interfere with the catalytic His-52, which is still present in this enzyme.

The CcP double mutants have reduced activity compared to CcP(W51H), and we suggest that a second factor contributes to slowing the reaction with H_2O_2, the reduced catalytic efficiency of His-51 compared to His-52. CcP(W51H/H52W) is 5-fold less active than CcP(W51H), while CcP(W51H/H52L) is ~100-fold less active. It is interesting to note that the identity of the residue at position 52 causes a 20-fold difference in activity. This is most likely due to alteration of the hydrogen bonding network within the distal heme pocket depending upon whether a leucine or tryptophan residue is at position 52. The tryptophan side chain can hydrogen bond to water, while that of leucine cannot. While both mutations allow water to coordinate to the heme iron, the W51H/H52L mutant may be less efficient at deprotonation of the incoming H_2O_2, slowing its binding to the heme iron. It is difficult to assess the catalytic efficiency of His-51 in the CcP W51H double mutants since multiple factors are involved. However, the spectra of CcP(W51H) and CcP(W51H/H52L) are almost identical, and we can assume the fraction of five-coordinate heme enzyme is approximately the same, ~2%. If this is true, then His-51 catalyzes the activation of H_2O_2 ~100 times less efficiently than His-52, with a rate of $\sim 5 \times 10^5$ M^{-1} s^{-1} for the five-coordinate form of the mutant, compared to a rate of $\sim 5 \times 10^7$ M^{-1} s^{-1} for the five-coordinate form of rCcP.

Ortiz de Montellano and colleagues have performed similar studies with HRP (*9*, *28*, *30*). Mutations within the distal heme pocket of HRP do not appear to affect heme ligation, and this minimizes the problem of correcting for the inactive six-coordinate forms of the mutants. In the case of HRP, the observed rates of reaction with H_2O_2 can be used directly to assess the effect of relocating the distal histidine. HRP(F41H/H42A) is 300 times less reactive than native HRP (*28*), indicating that a histidine at position 41 is ~300-fold less efficient than the wild-type histidine at position 42. The 300-fold decrease in catalytic activity for His-41 is similar to the 100-fold decrease in catalytic efficiency we attributed to His-51 in CcP. Ortiz de Montellano and colleagues have also relocated the histidine to the arginine position in the distal heme pocket, residue 38 in HRP and residue 48 in CcP. Histidine at position 38 is much less effective in promoting the reaction between H_2O_2 and the heme iron in HRP than either His-41 or His-42. The HRP(R38H/H42V) mutant is $\sim 2 \times 10^4$ times less reactive than native HRP (*30*) and only approximately 80−160-fold more reactive than HRP(H42A) and HRP (H42V), two mutants that lack a distal histidine (*9*).

The studies on the relocation of the catalytic histidine within the distal heme pocket are consistent with the idea that the active sites in the peroxidases have been optimized for H_2O_2 activation. Moving the histidine to either the Arg site (position 38 in HRP) or the aromatic residue site (position 41 in HRP and position 51 in CcP) decreases the rate of reaction with H_2O_2. MetMb reacts with H_2O_2 to form a "Compound I-like" intermediate (*6*); however, it has not evolved to optimize this reactivity. Several studies have shown that the rate of reaction between H_2O_2 and metMb can be enhanced by specific mutations within the distal heme pocket as well as elsewhere within the molecule (*10*−*12*, *31*−*33*). Three single-site mutants have been reported

that increase the rate of reaction with H_2O_2. H64Q has been reported to increase the rate 3.2-fold (*10*), although a second study saw no enhancement (*31*). H64D is reported to increase the rate 50−70-fold, the largest increase reported to date (*32*). F46L enhances the H_2O_2 rate by a factor of 2.4 even though Phe-46 is not within the distal heme pocket (*33*). The F46L mutation was identified in an in vitro random mutagenesis study that was screened for increased peroxidase activity. Two double mutants, L29F/V68F (*31*) and F43H/H64L (*11*), have reported enhancements of 2.7- and 11-fold, respectively, with the latter specifically designed to move the distal histidine to a location within the heme pocket that better mimics the position of the distal histidine in the peroxidases. A third double mutant, F46L/I107F, was identified in the second round of random mutagenesis and enhanced the rate 4.9-fold (*33*). In the final two rounds of random mutagenesis, a triple mutant, T39I/F46L/I107F, and a quadruple mutant, T39I/K45D/F46L/I107K, that increased the H_2O_2 reaction rate by factors of 19 and 25, respectively, were identified (*33*). All of the mutations in the random mutagenesis study were on the distal side of the heme, although none of the sites are generally recognized as being within the distal heme pocket or having significant influence on the functional or spectroscopic properties of metMb.

Decay of Compound I Formed by the W51H Mutants. The decay of CcP(W51H) Compound I is distinctly different from the decay of wild-type CcP Compound I (*24*). Decay of yCcP Compound I is biphasic with an initial fast phase [$k_1^{decay} = (1.3 \pm 0.3) \times 10^{-3}$ s^{-1}] accounting for 20% of the total absorbance change and a slower phase [$k_2^{decay} = (2.9 \pm 0.6) \times 10^{-5}$ s^{-1}] accounting for 80% of the reaction. The initial phase is attributed to migration of the Trp-191 radical to alternative sites and the second phase to reduction of the Fe(IV) site in yCcP Compound I. Using the decay rate constants associated with the largest absorbance changes at 424 nm [~80% of the total absorbance change for both CcP(W51H) and yCcP] as a measure of the reduction of the Fe(IV)═O heme in Compound I, the Fe(IV) site in CcP(W51H) Compound I is ~500 times less stable than the Fe(IV) site in yCcP Compound I, while the W51H/H51L and W51H/H52W mutants are 1100- and 3000-fold less stable.

The second unusual aspect of the decay of CcP(W51H) Compound I is that the absorbance at 424 nm actually decreases below that of the native Fe(III) state of the enzyme and then recovers to that of the native state (Figure 6). All mutants containing the W51H alteration, CcP(W51H), CcP(W51H/H52L), and CcP(W51H/H52W), show this decrease in absorbance below that of the of the Fe(III) state before recovery to that of the Fe(III) state. We have observed this behavior only for the W51H mutants. The initial phase of Compound I decay in the W51H mutants is reduction of the Fe(IV)═O heme site, producing a protein-based radical species. If the radical species is near the Fe(III) heme group, it most likely perturbs the spectrum of the heme. A calculated difference spectrum between CcP Compound I and CcP Compound II shows a decrease of ~0.004 μM^{-1} cm^{-1} at 424 nm (*34*), the difference in absorbance of the Fe(IV) site with and without the Trp-191 radical. The amplitude of this perturbation is similar to the amplitudes of the second and third phases of the decay of CcP(W51H) Compound I (Figure 6), providing some support for the idea that the two slower decay phases represent the reduction of the radical site or migration of the radical away from the vicinity of the heme.

Binding of Cyanide to the CcP Mutants. At pH 6.0, the rate of binding of cyanide to yCcP is monophasic (*25*), while the rates of binding for the three W51H mutants are biphasic. The fast phase of the reaction with the W51H mutants is linearly dependent upon the cyanide concentration (Figures 9, S11, and S12), indicating that the fast phase is the bimolecular cyanide binding reaction. The slow, cyanide-independent phase (Figures 9, S11, and S12) is attributed to an isomerization within the enzyme.

Scheme 1

Enzyme isomerization can affect the apparent equilibrium dissociation constant for the cyanide complexes. If one compares the kinetically calculated equilibrium constant ($K_D^{kin} = k_d/k_a$) for the monophasic binding of cyanide to yCcP with the equilibrium constant determined from equilibrium measurements (K_D^{equil}), the two values are within experimental error (Table 4), confirming that binding of cyanide to yCcP is a simple bimolecular process. However, for the three W51H mutants, the value of K_D^{kin} is from 3 to 8 times larger than K_D^{equil} (Table 4). The discrepancy between K_D^{kin} and K_D^{equil} can be rationalized in terms of Scheme 1. In Scheme 1, the enzyme exists in two conformational states, E and E′, interconverting with rate constants k_i and k_{-i}. These two enzyme states are not the penta- and hexacoordinate forms but some other conformational equilibrium that affects the rate of cyanide binding. Under the experimental conditions used in this study, cyanide binding is faster than the conformational isomerization and k_{fast} and k_{slow} are given by eqs 2 and 3, respectively. The isomerization equilibrium constant is defined in eq 4. Likewise, K_D^{kin} and K_D^{equil} are given by eqs 5 and 6, respectively. The value of K_{iso} can be calculated from K_D^{kin} and K_D^{equil}, and the calculated values are included in Table 4.

$$k_{fast} = k_a[CN] + k_d \quad (2)$$

$$k_{slow} = k_i \quad (3)$$

$$K_{iso} = [E]/[E'] = k_i/k_{-i} \quad (4)$$

$$K_D^{kin} = k_d/k_a \quad (5)$$

$$K_D^{equil} = K_D^{kin} K_{iso}/(1 + K_{iso}) \quad (6)$$

The rate of cyanide binding, characterized by k_a, can be viewed as diffusional partitioning of HCN into the distal heme pocket, followed by ionization of HCN within the pocket and binding of the cyanide anion to the heme iron. For many heme proteins, the rate of ionization of HCN within the distal heme pocket appears to be a rate-controlling step for cyanide binding (*29*, *36*), and this seems to be the case for the CcP W51H mutants.

Conclusions. The data presented in this study, along with other studies cited from the literature, support the idea that the structure of the peroxidase distal heme pocket has evolved to optimize activation of H_2O_2 to form the oxidized enzyme intermediate known as Compound I. All known mutations in the distal heme pocket of the peroxidases tested to date decrease the rate of the H_2O_2 reaction (*37*). Even relatively small changes such as moving the ε-nitrogen of the distal histidine ~0.4 Å closer

to the heme iron and placing it in an orientation similar to that in catalase (*38*) decrease the rate of Compound I formation 300-fold as seen for CcP(W51H/H52W). There are at least two factors involved in decreasing the rate of reaction with H_2O_2, less efficient base catalysis due to relocation of the distal histidine and blockage of the heme iron due to water binding. It is estimated that water coordination to the heme iron decreases the rate by a factor of ~50, related to the fraction of enzyme in the hexacoordinate form, while relocation of the distal histidine from position 52 to 51 causes decreases on the order of 5−100-fold due to less efficient base catalysis of the binding of hydrogen peroxide to the heme iron.

SUPPORTING INFORMATION AVAILABLE

Figures showing the spectra of CcP(W51H), CcP(W51H/H52W), and their cyanide complexes, hydrogen peroxide kinetic data, and cyanide binding data. This material is available free of charge via the Internet at http://pubs.acs.org.

REFERENCES

1. Zamocky, M., Regelsberger, Jakopitsch, C., and Obinger, C. (2001) The molecular peculiarities of catalase-peroxidase. *FEBS Lett. 492*, 177–182.
2. Takano, T. (1977) Structure of myoglobin refined at 2.0 Å resolution. I. Crystallographic refinement of metmyoglobin from sperm whale. *J. Mol. Biol. 110*, 537–568.
3. Finzel, B. C., Poulos, T. L., and Kraut, J. (1984) Crystal structure of yeast cytochrome *c* peroxidase refined at 1.7-Å resolution. *J. Biol. Chem. 259*, 13027–13036.
4. Dolphin, D., Forman, A., Borg, D. C., Fajer, J., and Felton, R. H. (1971) Compounds I of catalase and horseradish peroxidase: π-cation radicals. *Proc. Natl. Acad. Sci. U.S.A. 68*, 614–618.
5. Erman, J. E., Vitello, L. B., Mauro, J. M., and Kraut, J. (1989) Detection of an oxyferryl porphyrin π-cation-radical intermediate in the reaction between hydrogen peroxide and a mutant yeast cytochrome *c* peroxidase: Evidence for tryptophan-191 involvement in the radical site of compound I. *Biochemistry 28*, 7992–7995.
6. King, N. K., Looney, F. D., and Winfield, M. E. (1964) Myoglobin free radicals. *Biochim. Biophys. Acta 88*, 235–236.
7. Erman, J. E., Vitello, L. B., Miller, M. A., and Kraut, J. (1992) Active-site mutations in cytochrome *c* peroxidase: A critical role for histidine-52 in the rate of formation of compound I. *J. Am. Chem. Soc. 114*, 6592–6593.
8. Erman, J. E., Vitello, L. B., Miller, M. A., Shaw, A., Brown, K. A., and Kraut, J. (1993) Histidine 52 is a critical residue for rapid formation of cytochrome *c* peroxidase compound I. *Biochemistry 32*, 9798–9806.
9. Newmyer, S. L., and Ortiz de Montellano, P. R. (1995) Horseradish Peroxidase His-42 → Ala, His-42 → Val, and Phe-41 → Ala Mutants. Histidine catalysis and control of substrate access to the heme iron. *J. Biol. Chem. 270*, 19438–19438.
10. Brittain, T., Baker, A. R., Butler, C. S., Little, R. H., Lowe, D. J., Greenwood, C., and Watmough, N. J. (1997) Reaction of variant sperm-whale myoglobins with hydrogen peroxide: The effects of mutating a histidine residue in the haem pocket. *Biochem. J. 326*, 109–115.
11. Matsui, T., Ozaki, S., Liong, E., Phillips, G. N.Jr., and Watanabe, Y. (1999) Effects of the location of distal histidine in the reaction of myoglobin with hydrogen peroxide. *J. Biol. Chem. 274*, 2828–2844.
12. Ozaki, S., Roach, M. P., Matsui, T., and Watanabe, T. (2001) Investigations of the role of the distal heme environment and the proximal heme iron ligand in peroxide activation by heme enzymes via molecular engineering of myoglobin. *Acc. Chem. Res. 34*, 818–825.
13. Savenkova, M. I., Satterlee, J. D., Erman, J. E., Siems, W. F., and Helms, G. L. (2001) Expression, purification, characterization, and NMR studies of highly deuterated recombinant cytochrome *c* peroxidase. *Biochemistry 40*, 12123–12131.
14. Takio, K., Titani, K., Ericsson, L. H., and Yonetani, T. (1980) Primary structure of yeast cytochrome *c* peroxidase II. The complete amino acid sequence. *Arch. Biochem. Biophys. 203*, 615–6299.
15. Teske, J. G., Savenkova, M. I., Mauro, J. M., Erman, J. E., and Satterlee, J. D. (2000) Yeast cytochrome *c* peroxidase expression in *Escherichia coli* and rapid isolation of various highly purified holoenzymes. *Protein Expression Purif. 19*, 139–147.
16. Fishel, L. A., Villafranca, J. E., Mauro, J. M., and Kraut, J. (1987) Yeast cytochrome *c* peroxidase: Mutagenesis and expression in *Escherichia coli* show tryptophan-51 is not the radical site in compound I. *Biochemistry 26*, 351–360.
17. Morar, A. S., Kakouras, D., Young, G. B., Boyd, J., and Pielak, G. J. (1999) Expression of ^{15}N-labeled eukaryotic cytochrome *c* in *Escherichia coli*. *J. Biol. Inorg. Chem. 4*, 220–222.
18. Pollock, W. B. R., Rosell, F. I., Twitchett, M. B., Dumont, M. E., and Mauk, A. G. (1998) Bacterial expression of a mitochondrial cytochrome *c*. Trimethylation of Lys72 in yeast iso-1-cytochrome *c* and the alkaline conformational transition. *Biochemistry 37*, 6124–6131.
19. Kolthoff, I. M., and Belcher, R. (1957) Hydrogen peroxide. In *Volumetric Analysis*, Vol. *3*, pp 75−76, Interscience, New York.
20. Nelson, D. P., and Kieslow, L. A. (1972) Enthalpy of decomposition of hydrogen peroxide by catalase at 25 °C (with molar extinction coefficients of H_2O_2 solutions in the UV). *Anal. Biochem. 49*, 474–478.
21. Berry, E. A., and Trumpower, B. L. (1987) Simultaneous determination of hemes a, b, and c from pyridine hemochrome spectra. *Anal. Biochem. 161*, 1–15.
22. Vitello, L. B., Erman, J. E., Miller, M. A., Mauro, J. M., and Kraut, J. (1992) Effect of Asp-235 → Asn substitution on the absorption spectrum and hydrogen peroxide reactivity of cytochrome *c* peroxidase. *Biochemistry 31*, 11524–11535.
23. Antonini, E., and Brunori, M. (1971) in *Hemoglobin and myoglobin in their reactions with ligands*, North-Holland Publishing Co., Amsterdam.
24. Erman, J. E., and Yonetani, T. (1975) A kinetic study of the endogenous reduction of the oxidized sites in the primary cytochrome *c* peroxidase-hydrogen peroxide compound. *Biochim. Biophys. Acta 393*, 350–357.
25. Erman, J. E. (1974) Kinetic and equilibrium studies of cyanide binding by cytochrome *c* peroxidase. *Biochemistry 13*, 39–44.
26. Smith, D. W., and Williams, R. J. P. (1968) Analysis of the visible spectra of some sperm-whale ferrimyoglobin derivatives. *Biochem. J. 110*, 297–301.
27. Iizuka, T., and Yonetani, T. (1970) Spin changes in hemoproteins. *Adv. Biophys. 1*, 157–182.
28. Savenkova, M. I., Newmyer, S. L., and Ortiz de Montellano, P. R. (1996) Rescue of His-42 → Ala horseradish peroxidase by a Phe-41 → His mutation: Engineering of a surrogate catalytic histidine. *J. Biol. Chem. 271*, 24598–24603.
29. Brancaccio, A., Cutruzzolá, F., Allocatelli, C. T., Brunori, M., Smerdon, S. J., Wilkinson, A. J., Dou, Y., Keenan, D., Ikeda-Sato, M., Brantley, R. E.Jr., and Olson, J. S. (1994) Structural factors governing azide and cyanide binding to mammalian metmyoglobins. *J. Biol. Chem. 269*, 13842–13853.
30. Savenkova, M. I., Kuo, J. M., and Ortiz de Montellano, P. R. (1998) Improvement of peroxygenase activity by relocation of a catalytic histidine with the active site of horseradish peroxidase. *Biochemistry 37*, 10828–10836.
31. Alayash, A. I., Ryan, B. A. B., Eich, R. F., Olson, J. S., and Cashon, R. E. (1999) Reactions of sperm whale myoglobin with hydrogen peroxide: Effects of distal pocket mutations on the formation and stability of the ferryl intermediate. *J. Biol. Chem. 274*, 2029–2037.
32. Wan, L., Twitchett, M. B., Eltis, L. D., Mauk, A. G., and Smith, M. (1998) *In vitro* evolution of horse heart myoglobin to increase peroxidase activity. *Proc. Natl. Acad. Sci. U.S.A. 95*, 12825–12831.
33. Matsui, T., Ozaki, S., and Watanabe, Y. (1999) Formation and catalytic roles of compound I in the hydrogen peroxide-dependent oxidations by His64 myoglobin mutants. *J. Am. Chem. Soc. 121*, 9952–9957.
34. Coulson, A. F. W., Erman, J. E., and Yonetani, T. (1971) Studies on cytochrome *c* peroxidase. XVII. Stoichiometry and mechanism of the reaction of compound ES with donors. *J. Biol. Chem. 246*, 917–924.
35. Pearl, N. M., Jacobson, T., Arisa, M., Vitello, L. B., and Erman, J. E. (2007) Effect of single-site charge-reversal mutations on the catalytic properties of yeast cytochrome *c* peroxidase: Mutations near the high-affinity cytochrome *c* binding site. *Biochemistry 46*, 8263–8272.
36. Dou, Y., Olson, J. S., Wilkinson, A. J., and Ikeda-Saito, M. (1996) Mechanism of hydrogen cyanide binding to myoglobin. *Biochemistry 35*, 7107–7113.
37. Erman, J. E., and Vitello, L. B. (2002) Yeast cytochrome *c* peroxidase: Mechanistic stdies via protein engineering. *Biochim. Biophys. Acta 1597*, 193–220.
38. Fita, I., and Rossman, M. G. (1985) The active center of catalase. *J. Mol. Biol. 185*, 21–37.